Organic Chemistry Frontiers

ARTICLE

1D alignment of proteins and other nanoparticles by using reversible covalent bonds on cyclic peptide nanotubes

Juan M. Priegue, Iria Louzao, Iván Gallego, Javier Montenegro,* Juan R. Granja*

Received 00th January 20xx,
Accepted 00th January 20xx

DOI: 10.1039/x0xx00000x

www.rsc.org/

Self-assembling cyclic peptide nanotubes are supramolecular structures whose diameter and external surface properties are precisely controlled. In this communication we describe a general strategy to align different molecules on top of the nanotube surface by using cyclic peptides bearing chemoreversible reactive groups. *D,L*-α-cyclic peptides endowed with a hydrazide moiety were condensed with a pyrenecarboxyaldehyde to facilitate the nanotube formation and deposition on flat unfunctionalized surfaces. The hydrazide moieties can be liberated without affecting the tubular structure and then used to align on top of the nanotube other molecules bearing aldehyde functions. Additionally, the attachment of specific ligands allowed the supramolecular alignment of corresponding receptors, such as mannosyl aldehyde and concavaline-A, driven by the nanotube structure through complemetary protein-ligand interaction.

Introduction

Protein-based supramolecular assembling into periodic structures with different morphologies still represents a major challenge nowadays.[1] Besides a characteristically high structural durability that facilitates their recycling, the peptide linkages ensure an adequate environmental biodegradability. Rectilinear assembling of proteins represents fundamental structure to provide linear multivalent templates for 1D directional functions.[2] In general, this strategy requires crystal engineering to design specific structural modifications that facilitate protein assembly. One step further is the protein 1D-directed alignment on surfaces with a decisive precision for the development of chips, sensors, or the exploration of quantum physics at the nanoscale. Carbon nanotubes and DNA origamis have been used as templates for protein immobilization, but they still lack controlled mass fabrication and must be designed for each specific protein.[3]

Peptide nanotubes represent a very attractive alternative for this purpose.[4] They can be created from different type of peptides, allowing to tune the nanotube external properties and the interaction with different surfaces and proteins. Among the variety of nanotubes those made of cyclic peptides (self-assembling cyclic peptide nanotubes, SCPNs) of alternating chirality (***D,L*-α-CP**) represent one of the most promising materials because of the precise control of nanotube diameter and external surface properties (**Fig. 1**).[5] These structures have

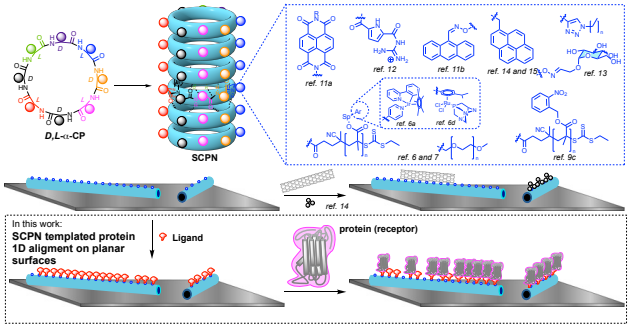

Figure 1. Cyclic peptide nanotubes previous strategies and precedents por deposition of different materials and this work approach.

unique properties as the precise control of nanotube diameter or the simple tuning of assembly properties. In the last years, several new contributions have shown the potential to impart novel features and functions of these materials based on the simplicity to exchange the residues used in the cyclic peptides (CPs) to tune SCPN surface properties. The incorporation of different type and number of polymer chains has been used to prepare advanced materials and biomedical applications.[6,7,8] Stimuli responsive nanotubes have also been described to mimic relevant biological functions such as cytoskeleton properties and so on.[9] Additionally, the rearrangement from one-dimensional self-assembly to bilayers able to form large nanosheets in the mesoscale driven by a specific sequence design have also been approached very recently.[10] In addition, the chemical transformations of some residues side chains have expanded their potential applications.[11] In this sense, the incorporation of naphtalenediamide on Lys side chains has been used to redox-triggered the formation with highly delocalized electronic states.[11a] Alternatively, the used of Lys rich CPs in which one residue was modified with a guanidiniocarbonylpyrrole moiety have been used for in cell

Singular Research Centre in Chemical Biology and Molecular Materials, (CIQUS), Organic Chemistry Department, University of Santiago de Compostela (USC), 15782 Santiago de Compostela, Spain.
† Footnotes relating to the title and/or authors should appear here.
Electronic Supplementary Information (ESI) available: [details of any supplementary information available should be included here]. See DOI: 10.1039/x0xx00000x

delivery of DNA.[12] Recently, click chemistry transformations have been used to incorporate not only polymers, but also alkyl chains to provide antimicrobial activity based on their membrane disrupting properties.[13]

In the last years, we have used a pyrene moiety attached to CPs, not only as a molecular probe to follow the assembling process, but also to supramolecularly interact with other molecules, such as single wall carbon nanotubes or small silver clusters in the fabrication of new hybrid materials (**Fig. 1**).[14] A similar strategy was used to generate a hierarchical process from CPs to fibers by the interdigitation of the aryl moieties. [11b,15] In this way, gel-like materials whose structure resemble those of cell-like cytoskeleton were prepared. Therefore, SCPNs have been used to direct and align the deposition of different materials on surfaces.[14] Unfortunately, they require aromatic "paddles" that can only interact with other aromatic or hydrophobic moieties in a non-specific manner, restricting their general application as templates for molecular alignment.

Therefore, SCPNs whose dimension and properties are easily tuned can arise as very valuable tool for exploring their ability to align different kind of materials at the nano scale. It is clear, considering the mentioned precedents, that the use of a more general (universal) recognition element would be very useful to extend this approach to other nanostructures such as proteins. Consequently, we envisage to develop a dynamic process in which the pyrene moiety is only temporally used to stabilize and induce nanotube formation (**Scheme 1**), but latter exchanged for other recognition elements. For this purpose, the use of covalent reversible bonds should allow to carry out this dynamic process by eliminating the aromatic moiety to liberate the reactive group that could be used to interact with different molecular pendants.[16] The initial peptide (with the attached pyrene) should assemble and deposited on appropriate surfaces such as mica.[11b,15] A key aspect is the use of covalent reversible bonds whose cleavage can be carried out under mild conditions without affecting the nanotube structure.[16] The resulting reactive ends would provide a new class of "molecular touch fasteners (velcro)" for the direct deposition of a broad diversity of suitable molecular counterparts. The precise tuning of nanotube structure allows to place the nanotube recognition groups on the solvent exposed surface, by placing these reactive ends at the opposite site of residue that direct SCPN deposition, i.e., residues with the same chirality placed at position 1 and 5 of the CP. This organization should permit the ligand exchange to attach other functions able to selectively interact with target moieties.

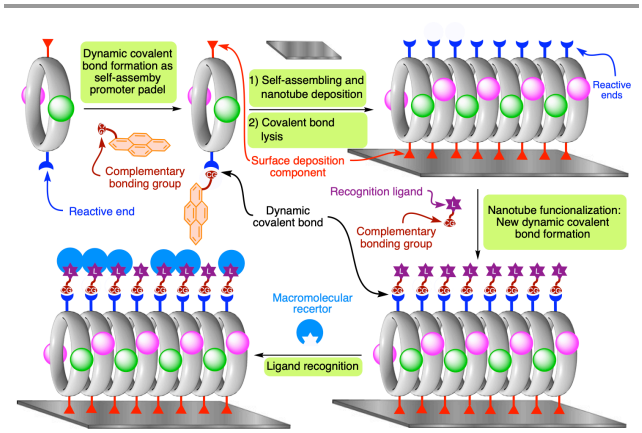

Scheme 1. General strategy for development of a universal tool for the deposition of different type of macromolecules on top of peptide nanotubes.

Results and discussion

Design concepts

Based on the previously mentioned hypothesis, cyclic peptide **CP1** (**Scheme 2**) was designed following similar principles used in our earlier work.[11b,15] Glu and Lys residues were incorporated to establish mutually attractive electrostatic interactions (ion-pairing) along the tube. The hydrazide moiety, placed at the opposite side of Arg, would be used as reactive end and

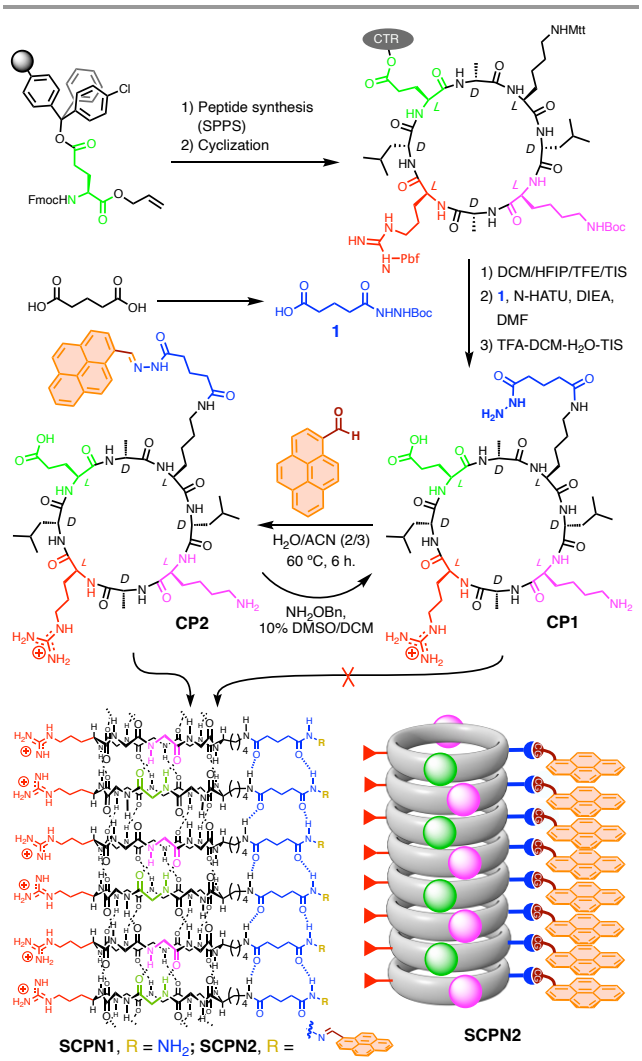

Scheme 2. Synthetic scheme used for the preparation of cyclic peptides described in this work in which the pyrene moiety was incorporated after the solid phase synthesis of **CP1** by hydrazone formation with pyrenecarboxyaldehyde to provide **CP2**. The self-assembling process of this CP gave rise to supramolecular structure **SCPN2** while the direct assembling of **CP1** did not provide the corresponding nanotube (**SCPN1**).

promotor of dynamic covalent bonds by condensation with appropriate aldehydes. This would allow the attachment of the pyrene moiety (self-assembling helper) and latter other ligands bearing a carbonyl moiety for substrate recognition (**Fig. 1**). The stacking of aromatic rings (π-π stacking) and salt bridges formation together with electrostatic interactions with the anionic surface of mica should align all the Arg side chains along the nanotube, facilitating its deposition.

Synthetic studies and characterization

Cyclic peptide **CP1** was prepared (**Scheme 2 and S1**) on solid support by attaching the side chain of Glu to the polystyrene resin (**CTR**, ChloroTrityl-Resin).[17] The proposed method allows not only the peptide cyclization prior to the cleavage but also the sidechain functionalization to incorporate the hydrazide moiety.[15] The Glu and Lys were used to facilitate the nanotube formation by favoring the antiparallel β-sheet type interactions between peptide rings.[18] After completing the synthesis of the linear octamer, the N- and C-terminal protecting groups, Fmoc and allyl, respectively, were removed and then cyclized on the solid support. After this, the methyltrityl protecting group (Mtt) of Lys side chain was removed by treatment with a mixture of hexafluoroisopropanol and trifluoroethanol[15] and then glutaric acid derivative **1** was coupled under standard conditions. Finally, the peptide was cleaved from the resin and purified by reverse phase HPLC. The condensation with 1-pyrenecarboxyaldehyde was carried out by heating at 60 °C the solution resulting of dissolving **CP1** in acetic acid and then added to a mixture of acetonitrile and water (3:2) containing the pyrene moiety to afford the final cyclic peptide **CP2** (see supporting information).

The assembling properties of **CP2** were clearly established by the fluorescence emission of the pyrene moiety. Vis-UV fluorescence spectra of aqueous solutions of **CP2** (**Fig. S1**) showed the typical features of the pyrene excimer band at ~465 nm that confirmed the close proximity of aryl moieties that can be related with the in solution assembling of this CP.[19] Interestingly, the excimer band is already observed at very low peptide concentration (0.5 μM), supporting the existence of nanotubes at quite low CP concentration. At 200 μM most of the peptide is already assembled into the nanotubes **SCPN2**, considering that most of the pyrene moieties are emitting as the

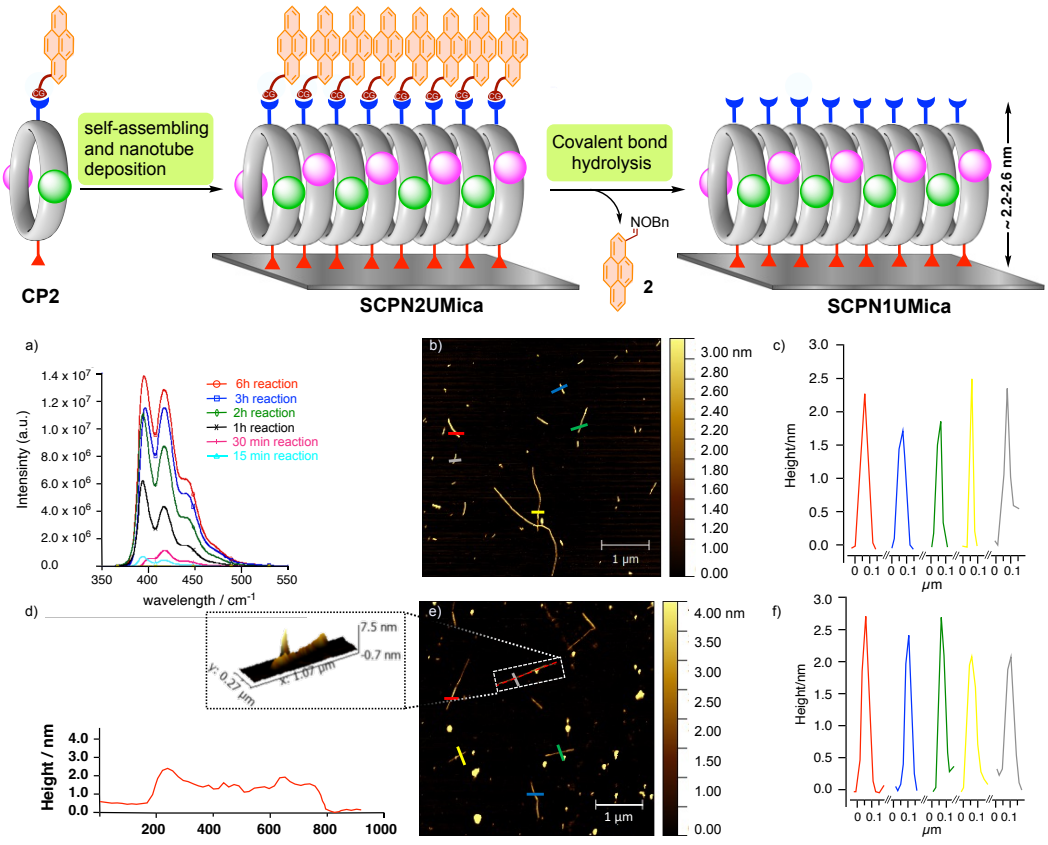

Figure 2. Studies of nanotube deposition on mica surface. **CP2** self-assembles into the tubular structure by the formation of hydrogen bonds between peptide backbone functions, assisted by the pyrene stacking. The resulting nanotubes align Arg side chains facilitating the electrostatic interactions with anionic surface of mica (**SCPN2UMica**). This arrangement leaves all the pyrene moieties disposed on top of the nanotube whose hydrolysis with O-benzylhydroxylamine, which followed by the UV emission of *O*-benzyl oxime of pyrene-1-carbaldehyde (**2**) at different reaction times (a), in cyan 15 min, magenta 30 min, black 1 h, dark green 2h, blue 3 h and red 6 h, to liberate the hydrazide function providing **SCPN1UMica**. b) AFM topography micrograph of **SCPN2UMica** (Grade V-I muscovite) from aqueous solutions 10 μM and (c) the corresponding height profiles along the transects in different colors shown in (b). (d) Magnified, top, 3D topographic image and of single nanotube from (e) and, bottom, observed profile along the tube longitudinal axis (red dotted line). (e) AFM topography micrograph of **SCPN1UMica** (Grade V-I muscovite) after hydrazone hydrolysis and (f) the corresponding height profiles along the transects in different colors shown in (e).

excimeric aggregate. This provides an association constant larger than any other previously reported CPs.[5,9,10,13] This can be related to the additional formation of two hydrogen bonds between the glutaric acid spacers (see model in **Scheme 2**).

Nanotube visualization on mica surface was next evaluated. For this purpose, solutions of **CP2** (1-650μM) in a mixture of ACN/H_2O (3:2) were placed on a mica surface and removed after 1h. The resulting surface was copiously washed with Milli-Q water and dried under nitrogen flow. AFM topographic imaging (**Fig. 2b-c** and **S2**) showed tubular structures lying horizontally on the surface with heights of 2.38±0.42 nm that matched with the expected nanotube diameter. The length and number of nanotubes clearly depend on CP concentration (**Fig. S2**). The good ability of this CP to self-assemble was supported by the observation of long **SCPNs** even at concentrations as low as 1 μM (**Fig. S2E**).

On surface SCPN functionalization (**Scheme S2**)

The next step was the optimization of the removal of the pyrene moiety that must take place without disrupting the deposited nanotubes. For this reason, we started searching for in-solution mild conditions using non-aqueous media that could be compatible with nanotube integrity. We found that the treatment of a solution of **CP2** with O-benzylhydroxylamine (BHA), independently of using mixture of organic solvents, transformed **CP2** into **CP1** in almost quantitative yield (**Fig. 2**). Next, we embark on the liberation of hydrazide groups on the deposited nanotubes. For this purpose, the mica plates containing the deposited peptide nanotubes (**SCPN2UMica)** were placed into a vial and immersed in a solution of BHA (100 mM) in different solvent mixtures. The micas were shaken for 6h and then analyzed by AFM. To do this, the micas were previously washed with dichloromethane and water before the AFM analysis. We found that the use of acetonitrile, DMSO or DMF gave rise mainly to the disappearance of nanotubes from the mica surface, while methanol, dichloromethane or water provided micas in which most nanotubes remained intact. The mica surfaces were in some areas dirty, having amorphous materials attached on them, probably related with the deposition of the *O*-benzyl oxime of pyrene-1-carbaldehyde (**2**, **Fig. 2**), but also with some CPs that were removed from the nanotube during the deprotection and washes steps or form the adhesive used to attach the micas to the microscope holder. Increasing the time or number of washes did not improve their cleaning. With the aim of enhancing the cleanliness of the surface, new solvent combinations were evaluated. We finally find out that the use of 10% of DMSO in dichloromethane (100 mM of BHA, 1mL) and washes with the same solvent mixture followed by thorough rinsing with Milli-Q water and subsequent drying under nitrogen flow, provided cleaner micas with intact nanotubes attached to the surface. The topographic images confirmed the integrity of the tubular structures (**Fig. 2e-f** and **4S**).

After optimizing the solvent mixture, we tuned other parameters, such as time or repetition number, required to release **2** resulting of the hydrazide liberation. The reaction was followed by UV-Vis using the characteristic emission band of pyrene moiety, see **Fig. 2a** regarding the reaction time and **Fig. S3** with respect to the number of mica immersions on the benzylhydroxylamine solution. Although after 12h most of the pyrene was already removed as denoted by the UV-Vis spectra (**Fig. 2a**), for all the following studies we leaved the samples immersed in the hydroxylamine solution for 24h. The micas were then washed several times with a DCM/DMSO (9:1) and analyzed by AFM, the heights (**Fig. 2e-f** and **Fig. S4**) were slightly

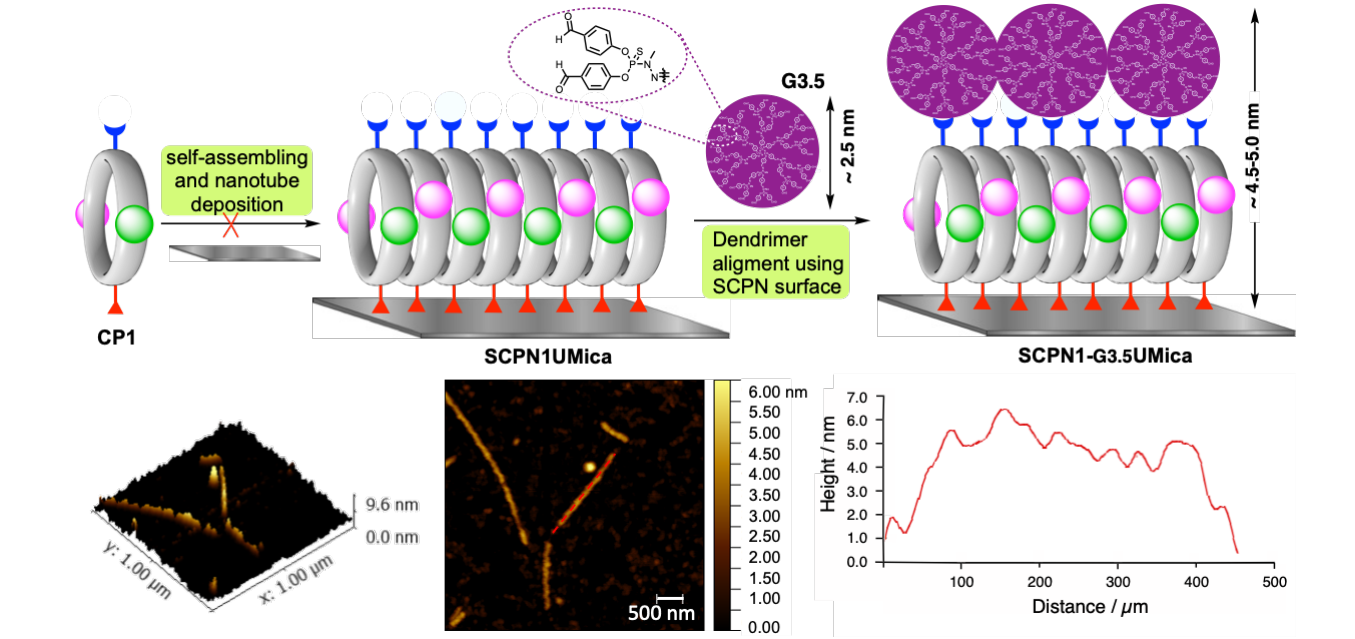

Figure 3. Formation of **SCPN1-G3.5UMica** by condensation of the **SCPN1UMica** with poly(phosphorhydrazone) dendrimer (**G3.5**, for the full structure see **Fig. S6**). AFM topography micrograph (Grade V-I muscovite) of this structure deposited over mica and on the right the corresponding height profile of the tube longitudinal axis (red dotted line) in which the increase of heights (~4.5 nm) by the attachment of dendrimer can be observed. On the left 3D topographic image.

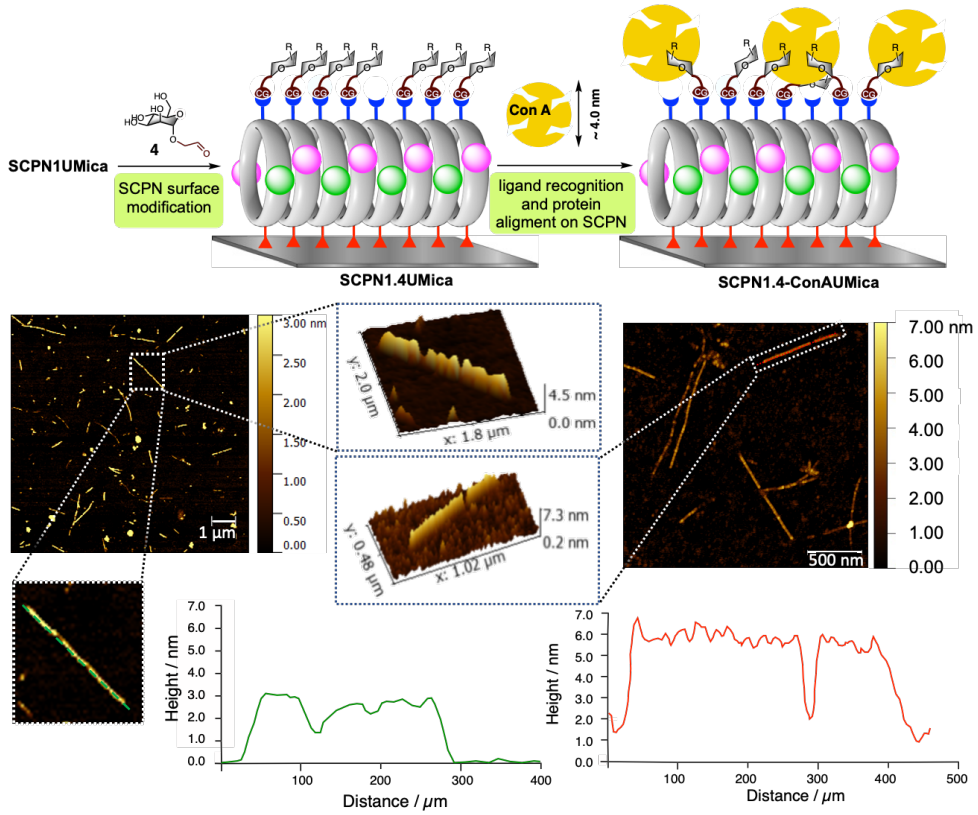

Figure 4. Strategy for the concavaline A (ConA) deposition on top of peptide nanotubes. The nanotubes deposited on the mica surface (**SCPN1UMica**) having the free hydrazyde after the benzylhydroxylamine treatment were treated with the mannosyl derivative **4** (**SCPN1.4UMica**). The resulting tubes having the saccharide moieties exposed on the surface were then treated with a solution of ConA (20 µM) to deposit it on top of the peptide nanotubes (**SCPN1.4UMica**). AFM topography micrograph of this samples (**SCPN1.4UMica**, on left and **SCPN1.4-ConAUMica** on the right) are shown with the corresponding magnified 3D topographic image of single nanotube of each sample. On the bottom, the observed profiles along the tube longitudinal axis (red dotted line) in different colors heights for these samples are also shown and they match with the proposed for these structures.

smaller (~2 nm) than those observed for the **SCPN2UMica** (**Fig. 2b-c** and **S3**). Statistical analysis of nanotube length (see table S1 in supporting information) after deprotection but also later on other mica modifications showed that there is not a significative change in nanotube length using these optimized conditions. It is worth mentioning that the direct mica deposition of pyrene-free CP (**CP1**) on the mica surface did not provide the expected tubular structures (**SCPN1UMica**), instead spherical nanoparticles with heights of 6.0 nm were obtained (**Fig. S5**). These experiments confirmed the requirement of pyrene moiety to facilitate the nanotube formation.

A direct condensation with a nano-sized aldehyde was then carried out to evaluate the reactivity of the free hydrazides. For this purpose we employed the poly(phosphorhydrazone) dendrimer **G3.5**, which contains 24 carbonyl moieties at the periphery (**Fig. S6**).[20] This dendrimer, with an estimated diameter of 2.5 nm, was nicely deposited on top of the nanotube as can be inferred form the AFM topographic images (**Fig. 3** and **S6**). To do that, the mica with the nanotubes bearing free hydrazide groups (**SCPN1UMica**) were treated with a solution of **G3.5** (10µM) in dichloromethane at room temperature. After the corresponding washed with DCM, the surface was evaluated by AFM, showing again long fibers, but with heights of 5.75±0.49 nm (**Fig. 3** and **Fig. S6**). These new heights match quite well with the expected for this type of structure (**SCPN1-G.35UMica**). Control experiments imaging mica surfaces with nanotubes bearing the pyrene moiety (**SCPN2UMica**) or mica surfaces in the absence of nanotubes did not provide similar results (**Fig. S7A and S7D**), confirming the requirement of hydrazide groups in order to condensate with the carbonyl groups of **G3.5** to address the deposition and alignment of the dendrimer guided by the nanotube.

Supramolecular functionalization of nanotubes for protein deposition

The potential of protein alignment using the nanotubular template was addressed by exploiting the supramolecular interaction between the concanavalin A (ConA) lectin and its natural α-mannosyl ligand.[21,22] Therefore, the free hydrazide nanotubes supported on mica surface (**SCPN1UMica**) were functionalized with an aldehyde bearing the β-mannosyl moiety. The insolubility of **4** in organic solvents compatible with nanotube structure force us to search for new condensation conditions. Finally, we found that the treated of **SCPN1UMica** with a solution of mannose-functionalized acetaldehyde (**4**, 5 µM)[23] in H_2O for 6 h (**Fig. 4**), followed by washing with water, provided nanotube structures that were again analyzed by AFM (**Fig. 4** and **Fig. S8**). The topography images confirmed the

integrity of the nanotubes with heights (**Fig. S8**) and lengths (**table S1**) similar to those of the original tubes **SCPN2UMica** (2.58±0.29 nm and 1.6 µm, respectively). In this case, the mica surface presented certain impurities, probably due to the successive manipulations and the use of aqueous media for the condensation reaction. Once the monosaccharide was attached to the nanotube, the resulting mica was treated with ConA in HEPES-buffered Krebs-Ringer solution (HKR). The topology characterization was again carried out by AFM, showing nanotubes with heights of 6.44±0.59 nm (**Fig. 4** and **Fig. S9-S10**) which were consistent with the expected size of a templated assembly between the peptide nanotubes (2-2.5 nm) and the ConA (4.0 nm).[24] Similar treatment of pristine micas or micas containing the peptide nanotubes with pyrene (**SCPN2UMica**) or the free hydrazide groups (**SCPN1UMica**) with the ConA solution did not give any substantial modification on the heights of the nanotubes (**Fig. S7**). This confirmed the importance of the α-mannosyl moiety attached to the nanotube for the ConA specific recognition and one-dimensional templated deposition.

Conclusions

We have implemented dynamic covalent bond procedure for 1D templated deposition using cyclic peptide nanotubes. The strategy is based on self-assembling peptide nanotubes bearing covalent dynamic bonds such as hydrazones. This strategy allowed protein controlled one dimensional deposition by using specific ligands that can be incorporated after nanotube installation through the reactive ends (hydrazide groups) bear by each cyclic peptide. The nanotubes were selectively deposited on the mica by the precise design of cyclic peptide component whose assembling process align on the same side of the nanotube specific functions. The incorporation of a pyrene group at the hydrazide moiety of CP induces the assembling process aligning all the guanidinium groups of Arg residues along the tube and, consequently, this facilitates the interaction with the mica surface. One can envision that this new modular approach could easily be adapted with other residue types and different surfaces. In addition, the use of dynamic covalent bonds, such as the hydrazone allows the controlled alignment of different functional groups at the nanoscale without affecting the nanotube integrity. In this regard, the nanotubes described here could also be used to align and deposit different proteins and receptors guided by the attached ligand. These hybrid biomaterials and this methodology could find applications in novel culture cell techniques, in catalysis, molecular storage, and drug delivery, among others.[2,13,25]

Acknowledgements

This work was supported by the Spanish Agencia Estatal de Investigación (AEI) and the ERDF (PID2019-111126RB-100, SAF2017-89890-R, EIG_JC2018-054), and by the Xunta de Galicia and the ERDF (ED431C 2017/25 and Centro singular de Investigación de Galicia accreditation 2019-2022, ED431G 2019/03). We also thank the ORFEO-CINCA network and Mineco (RED2018-102331-T). J.M.P. thanks to the Ministerio de Educación y Cultura (MEC) for his FPI contract. J.M. received an ISCIII (COV20/00297), ERC-Stg (DYNAP-677786), ERC-PoC (TraffikGene, 838002), and a YIG from the HFSP (RGY0066/2017).

Notes and references

1 a) H. Pyles, S. Zhang, J. J. D. Yoreo and D. Baker, Controlling protein assembly on inorganic crystals through designed protein interfaces, *Nature,* 2019, **571**, 251–256; b) J. Wang, H. Yu, X. Zhou, X. Liu, R. Zhang, Z. Lu, J. Zheng, L. Gu, K. Liu, D. Wang and L. Jiao, Probing the crystallographic orientation of two-dimensional atomic crystals with supramolecular self-assembly, *Nat. Commun.*, 2017, **8**, 377; c) G. Yang, L. Wu, G. Chen and M. Jiang, Precise protein assembly of array structures, *Chem. Commun.*, 2016, **52**, 10595–10605; d) H. Garcia-Seisdedos, C. Empereur-Mot, N. Elad and E. D. Levy, Proteins evolve on the edge of supramolecular self-assembly, *Nature*, 2017, **548**, 244–247, e) J. V. Barth, G. Costantini and K. Kern, Engineering atomic and molecular nanostructures at surfaces, *Nature*, 2005, **437**, 671–679.

2 a) C. Lv, X. Zhang, Y. Liu, T. Zhang, H. Chen, J. Zang, B. Zheng and G. Zhao, Redesign of protein nanocages: the way from 0D, 1D, 2D to 3D assembly, *Chem. Soc. Rev.,* 2021, **50**, 3957–3989; b) W. Zhang, S. Mo, M. Liu, L. Liu, L. Yu and C. Wang, Rationally designed protein building blocks for programmable hierarchical architectures, *Front. Chem.*, 2020, **8**, 587975; c) L. Miao, Q. Fan, L. Zhao, Q. Qiao, X. Zhang, C. Hou, J. Xu, Q. Luo and J. Liu, The construction of functional protein nanotubes by small molecule-induced self-assembly of cricoid proteins, *Chem. Commun.*, 2016, **52**, 4092–4095; d) A. Schreiber, M. C. Huber, H. C. O. lfen and S. M. Schiller, Molecular protein adaptor with genetically encoded interaction sites guiding the hierarchical assembly of plasmonically active nanoparticle architectures, *Nat. Commun.*, 2015, **6**, 6705.

3 a) C. M. Niemeyer, Nanoparticles, Proteins, and nucleic acids: Biotechnology Meets Materials Science, *Angew. Chem. Int. Ed.*, 2001, **40**, 4128–4158; b) K. Nagaraju, R. Reddy and N. Reddy, A review on protein functionalized carbon nanotubes, *J. Appl. Biomater. Funct. Mater.*, 2015, **13**, e301-e312; c) C. M. Niemeyer, T. Sano, C. L. Smith and C. R. Cantor, Oligonucleotide-directed self-assembly of proteins: Semisynthetic DNA–streptavidin hybrid molecules as connectors for the generation of macroscopic arrays and the construction of supramolecular bioconjugates, *Nucleic Acids Res*., 1994, **22**, 5530–5539; d) M. Calvaresi, and F. Zerbetto, The devil and holy water: Protein and carbon nanotube hybrids, *Acc. Chem. Res.*, 2013, **46,** 2454–2463; e) R. F. Hariadi, R. F. Sommese, A. S. Adhikari, R. E. Taylor, S. Sutton, J. A. Spudich and S. Sivaramakrishnan, Mechanical coordination in motor ensembles revealed using engineered artificial myosin filaments, *Nat. Nanotechnol.*, 2015, **10***,* 696–700.

4 a) T. Shimizu, W. Ding and N. Kameta, Soft-matter nanotubes: A platform for diverse functions and applications, *Chem. Rev.*, 2020, **120**, 2347–2407; b) N. C. Burgess, T. H. Sharp, F. Thomas, C. W. Wood, A. R. Thomson, N. R. Zaccai, R. L. Brady, L. C. Serpell and D. N. Woolfson, Modular design of self-assembling peptide-based nanotubes, *J. Am. Chem. Soc.*, 2015, **137**, 10554–10562; c) L. Adler-Abramovich and E. Gazit, The physical properties of supramolecular peptide assemblies: from building block association to technological applications, *Chem. Soc. Rev.*, 2014, **43**, 6881–6893; d) C. Xu, R. Liu, A. K. Mehta, R. C. Guerrero-Ferreira, E. R. Wright, S. Dunin-Horkawicz, K. Morris, L. C. Serpell, X. Zuo, J. S. Wall and

V. P. Conticello, Rational design of helical nanotubes from self-assembly of coiled-coil lock washers, *J. Am. Chem. Soc.*, 2013, **135**, 15565–15578; e) I. W. Hamley, Peptide nanotubes, *Angew. Chem. Int. Ed.*, 2014, **53**, 6866–6881; f) R. García-Fandiño, M. Amorín, J. R. Granja, Synthesis of Supramolecular Nanotubes, in *Supramolecular Chemistry: From Molecules to Nanomaterials*, ed. P. A. Gale and J. W. Steed, John Wiley & Sons Ltd, Chichester, UK, 2012, vol. 5, pp. 2149–2182.

5 a) N. Rodríguez-Vázquez, M. Amorín and J. R. Granja, Recent advances in controlling the internal and external properties of self-assembling cyclic peptide nanotubes and dimers, *Org. Biomol. Chem.,* 2017, **15**, 4490–4505; b) A. Fuertes, M. Juanes, J. R. Granja and J. Montenegro, Supramolecular functional assemblies: dynamic membrane transporters and peptide nanotubular composites, *Chem. Commun.,* 2017, **53**, 7861–7871; c) R. J. Brea, C. Reiriz and J. R. Granja, Towards functional bionanomaterials based on self-assembling cyclic peptide nanotubes, *Chem. Soc. Rev.*, 2010, **39**, 1448–1456; d) R Q. Song, Z. Cheng, M. Kariuki, S. C. L. Hall, S. K. Hill, J. Y. Rho and S. Perrier, Molecular self-assembly and supramolecular chemistry of cyclic peptides, *Chem. Rev.*, 2021, **121**, doi:10.1021/acs.chemrev.0c01291.

6 a) S. C. Larnaudie, J. C. Brendel, I. Romero-Canelón, C. Sanchez-Cano, S. Catrouillet, J. Sanchis, J. P. C. Coverdale, J.-I. Song, A. Habtemariam, P. J. Sadler, K. A. Jolliffe and S. Perrier, Cyclic peptide–polymer nanotubes as efficient and highly potent drug delivery systems for organometallic anticancer complexes, *Biomacromolecules*, 2018, **19**, 239–247; b) S. C. Larnaudie, J. C. Brendel, K. A. Jolliffe and S. Perrier, pH-responsive, amphiphilic core–shell supramolecular polymer brushes from cyclic peptide–polymer conjugates, *ACS Macro Lett.*, 2017, 1347–1351; c) J. Y. Rho, J. C. Brendel, L. R. MacFarlane, E. D. H. Mansfield, R. Peltier, S. Rogers, M. Hartlieb and S. Perrier, Probing the dynamic nature of self-assembling cyclic peptide–polymer nanotubes in solution and in mammalian cells, *Adv. Funct. Mater.*, 2017, **393**, 1704569; d) B. M. Blunden, R. Chapman, M. Danial, H. Lu, K. A. Jolliffe, S. Perrier, M. H. Stenzel, Drug conjugation to cyclic peptide–polymer self-assembling nanotubes, *Chem. Eur. J.* 2014, **20**, 12745–12749; e) G. Gody, D. A. Roberts, T. Maschmeyer and S. Perrier, A new methodology for assessing macromolecular click reactions and its application to amine-tertiary isocyanate coupling for polymer ligation, *J. Am. Chem. Soc.*, 2016, **138**, 4061–4068.

7 Q. Song, S. Goia, J. Yang, S. C. L. Hall, M. Staniforth, V. G. Stavros and S. Perrier, Efficient artificial light-harvesting system based on supramolecular peptide nanotubes in water, *J. Am. Chem. Soc.,* 2021, **143**, 382−389.

8 J. Yang, Ji-Inn Song, Q. Song, J. Y. Rho, E. D. H. Mansfield, S. C. L. Hall, M. Sambrook, F. Huang and S. Perrier, Hierarchical self-assembled photo-responsive tubisomes from a cyclic peptide-bridged amphiphilic block copolymer*, Angew. Chem. Int. Ed.,* 2020, **59**, 8860–8863.

9 a) N. Cissé and T. Kudernac, Light-fuelled self-assembly of cyclic peptides into supramolecular tubules, *Chemsystemschem*, 2020, **2**, e2000012; b) A. Méndez-Ardoy, A. Bayón-Fernández, Z. Yu, C. Abell, J. R. Granja and J. Montenegro, Spatially controlled supramolecular polymerization of peptide nanotubes by microfluidics, *Angew. Chem. Int. Ed.*, 2020, **59**, 6902–6908; c) M. Hartlieb, S. Catrouillet, A. Kuroki, C. Sanchez-Cano, R. Peltier and S. Perrier, Stimuli-responsive membrane activity of cyclic-peptide–polymer conjugates, *Chem. Sci.*, 2019, **10**, 5476–5483.

10 I. Insua and J. Montenegro, 1D to 2D self assembly of cyclic peptides, *J. Am. Chem. Soc.,* 2020, **142**, 300-307.

11 a) N. Ashkenasy, W. S. Horne and M. R. Ghadiri, Design of self-assembling peptide nanotubes with delocalized electronic states, *Small*, 2006, **2**, 99–102; b) F. Novelli, M. Vilela, A. Pazó, M. Amorín and J. R. Granja, Molecular plumbing to bend self-assembling peptide nanotubes, *Angew. Chem. Int. Ed.*, 2021, **60**, 18838–18844.

12 M. Li, M. Ehlers, S. Schlesiger, E. Zellermann, S. K. Knauer and C. Schmuck, Incorporation of a non-natural arginine analogue into a cyclic peptide leads to formation of positively charged nanofibers capable of gene transfection, *Angew. Chem. Int. Ed.*, 2016, **55**, 598–601.

13 E. González-Freire, F. Novelli, A. Pérez-Estévez, R. Seoane, M. Amorín and J. R. Granja, Double orthogonal click reactions for the development of antimicrobial peptide nanotubes, *Chem. Eur. J.*, 2021, **27**, 3029–3038.

14 a) M. Cuerva, R. García Fandiño, C. Vázquez-Vázquez, M. A. López-Quintela, J. Montenegro and J. Granja, Self-assembly of silver metal clusters of small atomicity on cyclic peptide nanotubes, *ACS Nano*, 2015, **9**, 10834–10843; b) J. Montenegro, C. Vázquez-Vázquez, A. Kalinin, K. E. Geckeler and J. R. Granja, Coupling of carbon and peptide nanotubes, *J. Am. Chem. Soc.*, 2014, **136**, 2484–2491.

15 a) A. Méndez-Ardoy, J. R. Granja and J. Montenegro, pH-triggered self-assembly and hydrogelation of cyclic peptide nanotubes confined in water micro-droplets, *Nanoscale Horiz.* 2018, **3**, 391–396.

16 a) E. Moulin, G. Cormos and N. Giuseppone, Dynamic combinatorial chemistry as a tool for the design of functional materials and devices, *Chem. Soc. Rev.*, 2012, **41**, 1031–1049; b) Y. Jin, C. Yu, R. J. Denman and W. Zhang, Recent advances in dynamic covalent chemistry, *Chem. Soc. Rev.*, 2013, **42**, 6634–6654; c) Y. Jin, Q. Wang, P. Taynton and W. Zhang, Dynamic covalent chemistry approaches toward macrocycles, molecular cages, and polymers, *Acc. Chem. Res.,* 2014, **47**, 1575–1586; d) M. Mastalerz, Permanent porous materials from discrete organic molecules—towards ultra-high surface areas. *Chem. Eur. J.*, 2012, **18**, 10082–10091; e) A. Herrmann, Dynamic combinatorial/covalent chemistry: a tool to read, generate and modulate the bioactivity of compounds and compound mixtures, *Chem. Soc. Rev.*, 2014, **43**, 1899–1933; f) J. Li, P. Nowak and S. Otto, Dynamic combinatorial libraries: From exploring molecular recognition to systems chemistry, *J. Am. Chem. Soc.,* 2013, **135**, 9222–9239; g) J. M. Priegue, D. N. Crisan, J. Martínez-Costas, J. Granja, F. Fernandez-Trillo and J. Montenegro, In situ functionalized polymers for siRNA delivery, *Angew. Chem. Int. Ed.*, 2016, **55**, 7618–7621.

17 a) J. M. Priegue, J. Montenegro and J. R. Granja, Single-nucleotide-resolution DNA differentiation by pattern generation in lipid bilayer membranes, *Small*, 2014, **10**, 3613–3618.

18 a) M. R. Silk, J. Newman, J. C. Ratcliffe, J. F. White, T. Caradoc-Davies, J. R. Price, S. Perrier, P. E. Thompson and D. K. Chalmers, Parallel and antiparallel cyclic *D/L* peptide nanotubes, *Chem. Commun.*, **2017**, *53*, 6613–6616; b) M. Calvelo, A. Lamas, A. Guerra, M. Amorín, R. García-Fandiño and J. R. Granja, Parallel versus antiparallel β-sheet structure in cyclic peptide hybrids containing γ- or δ-cyclic amino acids, *Chem. Eur. J.*, 2020, **26**, 5846–5858.

19 R. J. Brea, M. E. Vázquez, M. Mosquera, L. Castedo and J. R. Granja, Controlling multiple fluorescent signal output in cyclic peptide-based supramolecular systems, *J. Am. Chem. Soc.*, 2007, **129**, 1653–1657.

20 N. Launay, A. M. Caminade, R. Lahana and J. P. Majoral, A general synthetic strategy for neutral phosphorus-containing dendrimers, *Angew. Chem. Int. Ed. Engl.*, 1994, **33**, 1589–1592.

21 a) D. K. Mandal and C. F. Brewer, Differences in the binding affinities of dimeric concanavalin A (including acetyl and succinyl derivatives) and tetrameric concanavalin A with large oligomannose-type glycopeptides, *Biochemistry*, 1993, **32**,

5116–5120; b) C. P. Swaminathan, N. Surolia and A. Surolia, Role of water in the specific binding of mannose and mannooligosaccharides to concanavalin A, *J. Am. Chem. Soc.*, 1998, **120**, 5153–5159; c) H. Vedala, Y. Chen, S. Cecioni, A. Imberty, S. Vidal and A. Star, Nanoelectronic detection of lectin-carbohydrate interactions using carbon nanotubes. *Nano Lett.* 2011, **11**, 170–175; d) M.-E. Ragoussi, S. Casado, R. Ribeiro-Viana, G. de la Torre, J. Rojo and T. Torres, Selective carbohydrate–lectin interactions in covalent graphene- and SWCNT-based molecular recognition systems. *Chem. Sci.*, 2013, **4**, 4035–4041.

22 E. M. Muñoz, J. Correa, E. Fernández-Megía and R. Riguera, Probing the relevance of lectin clustering for the reliable evaluation of multivalent carbohydrate recognition, *J. Am. Chem. Soc.*, 2009, **131**, 17765–17767; M. Juanes, I. Lostalé-Seijo, J. R. Granja and J. Montenegro, Supramolecular recognition and selective protein uptake by peptide hybrids, *Chem. Eur. J.*, 2018, **30**, 10689–10698.

23 a) J. Reina, A. Rioboo and J. Montenegro, Glycosyl aldehydes: ew scaffolds for the synthesis of neoglycoconjugates via bioorthogonal oxime bond formation, *Synthesis*, 2018, **50**, 831–845; b) I. Gallego, A. Rioboo, J. J. Reina, B. Díaz, A. Canales, F. J. Cañada, J. Guerra-Varela, L. Sánchez and J. Montenegro, Glycosylated cell-penetrating peptides (GCPPs), *ChemBioChem*, 2019, **20**, 1400–1409.

24 G. N. Reeke, J. W. Becker, B. A. Cunningham, J. L. Wang, I. Yahara and G. M. Edelman, Structure and Function of Concanavalin A, in *Concanavalin A. Advances in Experimental Medicine and Biology*, T. eds. K. Chowdhury and A. K. Weiss, Springer, Boston, MA, 1975, vol. 55, pp 13–33.

25 a) Q. Luo, C. X. Hou, Y. S. Bai, R. B. Wang and J. Q. Liu, Protein assembly: Versatile approaches to construct highly ordered nanostructures, *Chem. Rev.,* 2016, **116**, 13571–13632; b) S. Abe, B. Maity and T. Ueno, Design of a confined environment using protein cages and crystals for the development of biohybrid materials, *Chem. Commun*., 2016, **52**, 6496–6512.

